

## Atomic layer deposition precursor step repetition and surface plasma pretreatment influence on semiconductor–insulator–semiconductor heterojunction solar cell

Florian Talkenberg, Stefan Illhardt, György Zoltán Radnóczy, Béla Pécz, Gabriele Schmidl, Alexander Schleusener, Kadyrjan Dikhanbayev, Gauhar Mussabek, Alexander Gudovskikh, and Vladimir Sivakov

Citation: *Journal of Vacuum Science & Technology A* **33**, 041101 (2015); doi: 10.1116/1.4921726

View online: <http://dx.doi.org/10.1116/1.4921726>

View Table of Contents: <http://scitation.aip.org/content/avs/journal/jvsta/33/4?ver=pdfcov>

Published by the AVS: Science & Technology of Materials, Interfaces, and Processing

### Articles you may be interested in

Tuning of undoped ZnO thin film via plasma enhanced atomic layer deposition and its application for an inverted polymer solar cell

*AIP Advances* **3**, 102114 (2013); 10.1063/1.4825230

Power losses in bilayer inverted small molecule organic solar cells

*Appl. Phys. Lett.* **101**, 233903 (2012); 10.1063/1.4769440

Growth morphology and electrical/optical properties of Al-doped ZnO thin films grown by atomic layer deposition



*J. Vac. Sci. Technol. A* **30**, 021202 (2012); 10.1116/1.3687939

Energy harvesting in semiconductor-insulator-semiconductor junctions through excitation of surface plasmon polaritons

*Appl. Phys. Lett.* **100**, 061127 (2012); 10.1063/1.3684833

Zn ( O , S ) buffer layers by atomic layer deposition in Cu ( In , Ga ) Se 2 based thin film solar cells: Band alignment and sulfur gradient

*J. Appl. Phys.* **100**, 044506 (2006); 10.1063/1.2222067

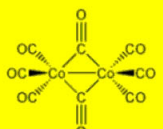
Corporate Headquarters  
Newburyport, MA USA

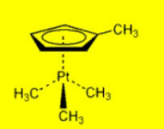
European Office  
Bischoheim, France

[Visit strem.com/cvd](http://strem.com/cvd)

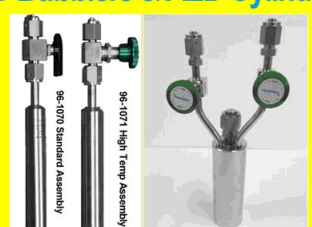
### Over 350 CVD & ALD Precursors

- metal alkyls
- metal alkoxides
- metal β-diketonates
- volatile organometallics
- electronic grade chemicals
- metal alkylamides
- metal amidinates
- volatile metal carbonyls
- fluorinated derivatives





### CVD Bubblers & ALD Cylinders



96-070 Standard Assembly

96-1071 High Temp Assembly

DOT and UN approved configurations available as well as precursor filling & refilling services.

# Atomic layer deposition precursor step repetition and surface plasma pretreatment influence on semiconductor–insulator–semiconductor heterojunction solar cell

Florian Talkenberg<sup>a)</sup> and Stefan Illhardt

*Leibniz Institute of Photonic Technology, Albert-Einstein-Str. 9, D-07745 Jena, Germany*

György Zoltán Radnóczy and Béla Pécz

*Centre for Energy Research, Institute of Technical Physics and Materials Science, Konkoly-Thege Miklós u. 29-33, H-1121 Budapest, Hungary*

Gabriele Schmidl and Alexander Schleusener

*Leibniz Institute of Photonic Technology, Albert-Einstein-Str. 9, D-07745 Jena, Germany*

Kadyrjan Dikhanbayev and Gauhar Mussabek

*Department of Physics and Engineering, al-Farabi Kazakh National University, 71 al-Farabi Ave., 050040 Almaty, Kazakhstan*

Alexander Gudovskikh

*Nanotechnology Research and Education Centre, St. Petersburg Academic University, Russian Academy of Sciences, Hlopina Str. 8/3, 194021 St. Petersburg, Russia*

Vladimir Sivakov

*Leibniz Institute of Photonic Technology, Albert-Einstein-Str. 9, D-07745 Jena, Germany*

(Received 25 February 2015; accepted 14 May 2015; published 27 May 2015)

Semiconductor–insulator–semiconductor heterojunction solar cells were prepared using atomic layer deposition (ALD) technique. The silicon surface was treated with oxygen and hydrogen plasma in different orders before dielectric layer deposition. A plasma-enhanced ALD process was applied to deposit dielectric Al<sub>2</sub>O<sub>3</sub> on the plasma pretreated n-type Si(100) substrate. Aluminum doped zinc oxide (Al:ZnO or AZO) was deposited by thermal ALD and serves as transparent conductive oxide. Based on transmission electron microscopy studies the presence of thin silicon oxide (SiO<sub>x</sub>) layer was detected at the Si/Al<sub>2</sub>O<sub>3</sub> interface. The SiO<sub>x</sub> formation depends on the initial growth behavior of Al<sub>2</sub>O<sub>3</sub> and has significant influence on solar cell parameters. The authors demonstrate that a hydrogen plasma pretreatment and a precursor dose step repetition of a single precursor improve the initial growth behavior of Al<sub>2</sub>O<sub>3</sub> and avoid the SiO<sub>x</sub> generation. Furthermore, it improves the solar cell performance, which indicates a change of the Si/Al<sub>2</sub>O<sub>3</sub> interface states. © 2015 American Vacuum Society. [<http://dx.doi.org/10.1116/1.4921726>]

## I. INTRODUCTION

The generation of electricity from sunlight by using photovoltaic technology and concentrated solar thermal power represent an essential pillar of future global energy production. The most common single crystalline silicon based solar cells produced by the industry today achieve at time conversion efficiencies over 20%. Other absorber materials like gallium arsenide (GaAs) or combinations of different absorber materials in multijunction solar cells promise the possibilities to increase conversion efficiency.<sup>1,2</sup>

However, the higher costs of these cell types make them currently uneconomic, in spite of their higher conversion efficiencies. The main challenge is to develop novel, cheaper solar cell concepts. The reduction of silicon in the cells is an obvious way to lower the cost. Another way is to use low-grade Si instead of ultrapure Si that is currently used. However, this lower-grade material is less efficient. It is presumed that the grid parity of solar cells will be reached by using thin-film technology or a new design that is

most-likely based on nanotechnology.<sup>3,4</sup> Solar cells with all sorts of nanoscale components have been widely investigated and summarized under the name third generation solar cells, in particular since high efficiencies can be accompanied by cost effectiveness of materials usage and production.<sup>5–10</sup>

p-n junctions in photovoltaics have a depth up to one or more micrometres. The uses of nanostructures and absorber layers with a thickness of a few micrometres contradict to the depth of the p-n junction.<sup>11,12</sup> The light absorption mainly occurs in the nanostructure, in lower depth. The use of heterojunctions like Si/a-Si:H,<sup>13</sup> Schottky barrier<sup>14</sup> or metal–insulator–semiconductor<sup>15,16</sup> are favorable. Semiconductor–insulator–semiconductor (SIS) is also a type of heterojunction, which was first developed in the 1970s and achieves theoretically a maximum conversion efficiency of 25%.<sup>17–19</sup>

A SIS junction consists of two semiconductors that are separated by a 1–3 nm thin dielectric layer. The charge carrier separation mechanism bases on a quantum mechanical tunneling of charge carriers through the dielectric barrier. SIS junctions were prepared by several methods. For

<sup>a)</sup>Electronic mail: [florian.talkenberg@iplt-jena.de](mailto:florian.talkenberg@iplt-jena.de)

example, silicon oxide ( $\text{SiO}_2$ ) was used as dielectric material. It was generated by thermal or unintentional oxidation of the silicon substrate during the deposition of the transparent conductive oxide (TCO). Typically, indium tin oxide (ITO) serves as TCO.<sup>18,20–24</sup>

Atomic layer deposition (ALD) is a modified chemical vapor deposition (CVD) technique and offers the possibility to deposit monolayer (ML) scale films of high uniformity, particularly on high aspect ratio structured surfaces.<sup>25,26</sup> Different conducting, semiconducting, and a large number of dielectric materials can be deposited by ALD.<sup>27–29</sup> Zinc oxide (ZnO) as well as aluminum doped zinc oxide (Al:ZnO or AZO) can also be deposited with high conductivity and high optical transmission by this technique and thus applied as TCO material.<sup>30</sup> The benefits in using of Al:ZnO instead of ITO in ALD are lower costs, the more simple precursor chemistry, and thus the easier realization of the ALD process.<sup>28</sup> The marginal deficit in conductivity of Al:ZnO compared to that of ITO is negligible in this case.<sup>31</sup> Thus, ALD is very suitable for producing SIS solar cells.

Even today only one publication about applying thermal ALD technique for SIS solar cell formation, while simultaneously testing different dielectric layers, can be found in literature. The highest conversion efficiency of 8% was achieved by using lanthanum oxide ( $\text{La}_2\text{O}_3$ ) as dielectric and Al:ZnO as front contact.<sup>32</sup> Before applying a SIS heterojunction on nanostructured surfaces for photovoltaics, a more detailed knowledge about how the ALD process parameters influence the SIS solar cell parameters is strongly required. Effects like precursor decomposition, fast desorption from the surface, and high temperature dependency to the deposited material structure (amorphous, polycrystalline, and monocrystalline) can disturb an ALD process and distort the results of SIS solar cell parameters.<sup>25</sup> The formation of  $\text{La}(\text{OH})_x$  can be observed during the deposition of  $\text{La}_2\text{O}_3$  using tris(*N,N'*-di-isopropyl formamidinate)lanthanum and water ( $\text{H}_2\text{O}$ ) as precursors. The self-limitation of the ALD process is disturbed by a desorption of  $\text{H}_2\text{O}$  from  $\text{La}(\text{OH})_x$ . The desorption leads to a parasitic CVD reaction.<sup>33,34</sup> This or other disturbing effects do not occur during the ALD growth of  $\text{Al}_2\text{O}_3$  using trimethylaluminum (TMA) and  $\text{H}_2\text{O}$  or  $\text{O}_2$  plasma as aluminum and oxygen precursors.<sup>35</sup> Up to now, high conversion efficiencies were not reached by using aluminum oxide ( $\text{Al}_2\text{O}_3$ ) as dielectric material in SIS junction.<sup>32</sup> Based on that, alumina is a useful dielectric material for fundamental SIS formation studies.

In this paper, we investigate the fundamental influences on the Si/ $\text{Al}_2\text{O}_3$  interface and on the SIS solar cell parameters by a plasma pretreatment of the silicon surface, which is performed immediately before the dielectric  $\text{Al}_2\text{O}_3$  deposition, and by the repetition of precursor dose steps during the  $\text{Al}_2\text{O}_3$  deposition. For  $\text{Al}_2\text{O}_3$  deposition, plasma-enhanced ALD (PE-ALD) was applied and for Al:ZnO thermal ALD. PE-ALD was selected because of lower leak current of  $\text{Al}_2\text{O}_3$  films compared to those of thermal ALD.<sup>36</sup> The dielectric layer in SIS junction can have a thickness below 1 nm, so the initial growth behavior of the dielectric is important. The aim of this paper is first to better understand the

initial growth behavior of the dielectric layer and how it affects the photovoltaic properties of solar devices and second to develop fundamental ALD process methods to improve the SIS junction.

## II. EXPERIMENT

Semiconductor–insulator–semiconductor heterojunction solar cells were realized on commercial phosphorus doped (100)-oriented n-type silicon wafers with a specific resistivity of 1–10  $\Omega\text{cm}$ . As deposition system a commercial ALD reactor (OpAL Oxford Instruments) was used, which is able to deposit films by thermal and by plasma-enhanced ALD. The plasma source of the ALD reactor is a remote plasma system and can generate oxygen and hydrogen radicals. The ALD reactor can perform a plasma pretreatment as well as deposition by thermal and plasma-enhanced methods in one process procedure.

The silicon substrate was equipped with a sputtered interface contact layer of 3 nm titanium and an aluminum back contact of 300 nm. A photoresist (AZ 1514H) was used to protect the aluminum back contact against hydrofluoric acid (HF). The native silicon oxide removal was carried out by a 1 min dip in 2% HF. After the HF dip, the photoresist was removed by dipping substrates for 1 min in acetone and 1 min in isopropanol. The substrates were rinsed in deionized water and blow-dried with nitrogen. Immediately the substrates are pretreated by plasma and covered with dielectric  $\text{Al}_2\text{O}_3$  and Al:ZnO by ALD at a temperature of 225 °C in one process.

The dielectric  $\text{Al}_2\text{O}_3$  layer, which act as barrier between silicon and Al:ZnO, was deposited by a plasma enhanced process where TMA was used as metal precursor and oxygen plasma as oxidizing reactant. Argon (Ar) and nitrogen ( $\text{N}_2$ ) served as purge gas. The  $\text{Al}_2\text{O}_3$  growth sequence was 50 ms TMA dose, 2 s Ar/ $\text{N}_2$  chamber purge, 2 s oxygen plasma (flow rate 50 sccm), and 2 s Ar/ $\text{N}_2$  chamber purge.

The deposition of Al:ZnO, which act as front contact, was performed by a thermal ALD process on top of dielectric  $\text{Al}_2\text{O}_3$  layer. If the plasma-enhanced instead of the thermal method would be used, then the Al:ZnO layer would be low or none conductive.<sup>37</sup> Diethylzinc (DEZ) and TMA act as metal precursors and deionized water ( $\text{H}_2\text{O}$ ) as oxygen agent. The ZnO growth sequence was 20 ms DEZ dose (exposure), 4 s Ar/ $\text{N}_2$  chamber purge, 20 ms  $\text{H}_2\text{O}$  dose and 7 s Ar/ $\text{N}_2$  chamber purge. The Al doping was realized by an  $\text{Al}_2\text{O}_3$  growth sequence of 10 ms TMA dose, 4 s Ar/ $\text{N}_2$  chamber purge, 30 ms  $\text{H}_2\text{O}$  dose, and 5 s Ar/ $\text{N}_2$  chamber purge. The growth of Al:ZnO was realized by performing one doping cycle of the  $\text{Al}_2\text{O}_3$  sequence after 20 cycles of the ZnO sequence (1:20), which represent one super cycle. Sixty super cycles of Al:ZnO (1:20) were deposited on top of the  $\text{Al}_2\text{O}_3$  layer. Spectroscopic ellipsometry and electric four point measurements show a Al:ZnO film thickness of 230 nm and a conductivity of approximately  $2 \times 10^{-3} \Omega\text{cm}$ .

In the first part of the investigation, the repetition of single precursor dose steps was performed. The precursor dose step and the chamber purge step of the metal precursor (TMA) and/or of oxidizing precursor were repeated five times. The following variations were performed: (i) “single

dose [1× TMA and purge, 1× O<sub>2</sub> plasma and purge] (H<sub>2</sub> plasma pretreatment)” (abbr.: SD[1×, 1×] (H<sub>2</sub> pl.)); (ii) “multidose [5× TMA and purge, 5× O<sub>2</sub> plasma and purge] (H<sub>2</sub> plasma pretreatment)” (abbr.: MD[5×, 5×] (H<sub>2</sub> pl.)); (iii) “multidose [5× TMA and purge, 1× O<sub>2</sub> plasma and purge] (H<sub>2</sub> plasma pretreatment)” (abbr.: MD[5×, 5×] (H<sub>2</sub> pl.)); and (iv) “single dose [1× TMA and purge, 1× O<sub>2</sub> plasma and purge] (no plasma pretreatment)” (abbr.: SD[1×, 1×] (no pl.)). The growth rate of Al<sub>2</sub>O<sub>3</sub> of all process variations is 0.11 nm/cycle. The number of cycles was altered between 1 and 20 cycles (Table I).

Because of the results in the first part, in the second part, only the TMA dose step and chamber purge step are repeated five times during the Al<sub>2</sub>O<sub>3</sub> deposition (MD[5×, 1×]). Before the deposition of Al<sub>2</sub>O<sub>3</sub>, a 15s plasma pretreatment with 10 sccm flow rate and a plasma power of 300 W was performed. Four types of pretreatments were performed: (1) “O<sub>2</sub> plasma” pretreatment; (2) “H<sub>2</sub> plasma” pretreatment; (3) “no plasma” pretreatment; (4) 15s O<sub>2</sub> plasma followed by 15s H<sub>2</sub> plasma pretreatment. The number of deposited Al<sub>2</sub>O<sub>3</sub> cycles of was variegated between 0 and 10 cycles (Table I).

The produced solar cells were diced on an area of 25 mm<sup>2</sup> (5 mm × 5 mm). Gold tips (diameter 0.45 mm) were directly brought in contact with aluminum back contact and Al:ZnO front contact. The current–voltage (I-V) characteristic was measured under dark and illuminated condition by a Sun simulator (AM1.5, 1000 W/m<sup>2</sup>, SS-80 PET). The solar cell parameters [open circuit voltage ( $V_{oc}$ ), short circuit current density ( $J_{sc}$ ), fill factor ( $FF$ ), and conversion efficiency ( $\eta$ )] were determined from I-V characteristic. The Si/Al<sub>2</sub>O<sub>3</sub> interface was investigated by transmission electron microscopy (TEM) [JEOL 3011 high resolution electron microscope with Gatan Imaging Filter (GIF Tridiem)].

### III. RESULTS AND DISCUSSION

#### A. Dose repetition

First, the influence of dose repetition during dielectric Al<sub>2</sub>O<sub>3</sub> deposition on SIS solar cells is reported. Figure 1 shows the solar cell parameters of four different dose

repetition cases against deposited Al<sub>2</sub>O<sub>3</sub> cycles. Open circuit voltage  $V_{oc}$  [Fig. 1(a)], short circuit current density  $J_{sc}$  [Fig. 1(b)], and  $FF$  [Fig. 1(c)] were determined from current–voltage (IV) measurement under Sun simulator. With these parameters, the cell area and the illumination density, the conversion efficiency  $\eta$  [Fig. 1(d)] is determined.

Most noticeable in solar cell parameters is  $V_{oc}$  [Fig. 1(a)]. A H<sub>2</sub> plasma pretreatment of silicon surface was performed except in case (iv) “SD[1×, 1×] (no pl.)”. The H<sub>2</sub> plasma pretreatment in case of (i) “SD[1×, 1×] (H<sub>2</sub> pl.)” lead to a bit higher and more continuous level of  $V_{oc}$  [Fig. 1(a)]. The comparison of (ii) “MD[5×, 5×] (H<sub>2</sub> pl.)” and (iii) “MD[5×, 1×] (H<sub>2</sub> pl.)” to (i) “MD[1×, 1×] (H<sub>2</sub> pl.)” shows a more pronounced difference. The repetition of TMA dose and oxygen plasma steps decreases  $V_{oc}$  to 260–280 mV as compared to none repetition. Repeating only the TMA dose step increases  $V_{oc}$  to 340–400 mV.

The short circuit current density  $J_{sc}$  does not show such a significant difference without (iv) SD[1×, 1×] (no pl.) [Fig. 1(b)]. The curves of (i) SD[1×, 1×] (H<sub>2</sub> pl.) ( $J_{sc} = 13$  mA/cm<sup>2</sup>), (ii) MD[5×, 5×] (H<sub>2</sub> pl.) ( $J_{sc} = 11$ –16 mA/cm<sup>2</sup>), and (iii) MD[5×, 1×] (H<sub>2</sub> pl.) ( $J_{sc} = 16$ –19 mA/cm<sup>2</sup>) show a strong decrease above 4 cycles and goes down to near zero at 10 cycles. The decrease in case (iv) SD[1×, 1×] (no pl.) ( $J_{sc} = 14$ –18 mA/cm<sup>2</sup>) is shifted to 8 cycles. The curve goes down to near zero at 16 cycles.

The  $FF$  in all cases is above 25% for less than 4 cycles [Fig. 1(c)]. Above 4 cycles, the fill factors of (i) SD[1×, 1×] (H<sub>2</sub> pl.), (ii) MD[5×, 5×] (H<sub>2</sub> pl.), and (iii) MD[5×, 1×] (H<sub>2</sub> pl.) decrease in the named order with different rate. The decrease in case (iv) SD[1×, 1×] (no pl.) is shifted to 8 cycles like for  $J_{sc}$  [Fig. 1(b)].

The behavior of solar cell conversion efficiency  $\eta$  is similar to that of  $J_{sc}$ . The maximum efficiencies are for (i) SD[1×, 1×] (H<sub>2</sub> pl.) 1.1%, (ii) MD[5×, 5×] (H<sub>2</sub> pl.) 1.2%, (iv) SD[1×, 1×] (no pl.) 1.4%, and for (iii) MD[5×, 1×] (H<sub>2</sub> pl.) 1.6%.

#### B. Plasma pretreatment

Second, the influence of different plasma pretreatments is reported. Pretreatments of (1) O<sub>2</sub> plasma, (2) H<sub>2</sub> plasma, (3)

TABLE I. SIS solar cell series and ALD process procedure overview.

Series caption	Plasma pretreatment	ALD process procedure				Front contact
		Cycles	Dielectric Al <sub>2</sub> O <sub>3</sub>			
			TMA	O <sub>2</sub> plasma		
(i) SD[1×, 1×] (H <sub>2</sub> pl.)	15s H <sub>2</sub>	1–20	1×	1×	Al:ZnO 230 nm	
(ii) MD[5×, 5×] (H <sub>2</sub> pl.)	15s H <sub>2</sub>	1–20	5×	5×		
(iii) MD[5×, 1×] (H <sub>2</sub> pl.)	15s H <sub>2</sub>	1–20	5×	1×		
(iv) SD[1×, 1×] (no pl.)	—	1–20	1×	1×		
(1) O <sub>2</sub> plasma	15s O <sub>2</sub>	0–10	5×	1×		
(2) H <sub>2</sub> plasma	15s H <sub>2</sub>	0–10	5×	1×		
(3) no plasma	—	0–10	5×	1×		
(4) O <sub>2</sub> and H <sub>2</sub> plasma	15s H <sub>2</sub> and 15s O <sub>2</sub>	0–10	5×	1×		



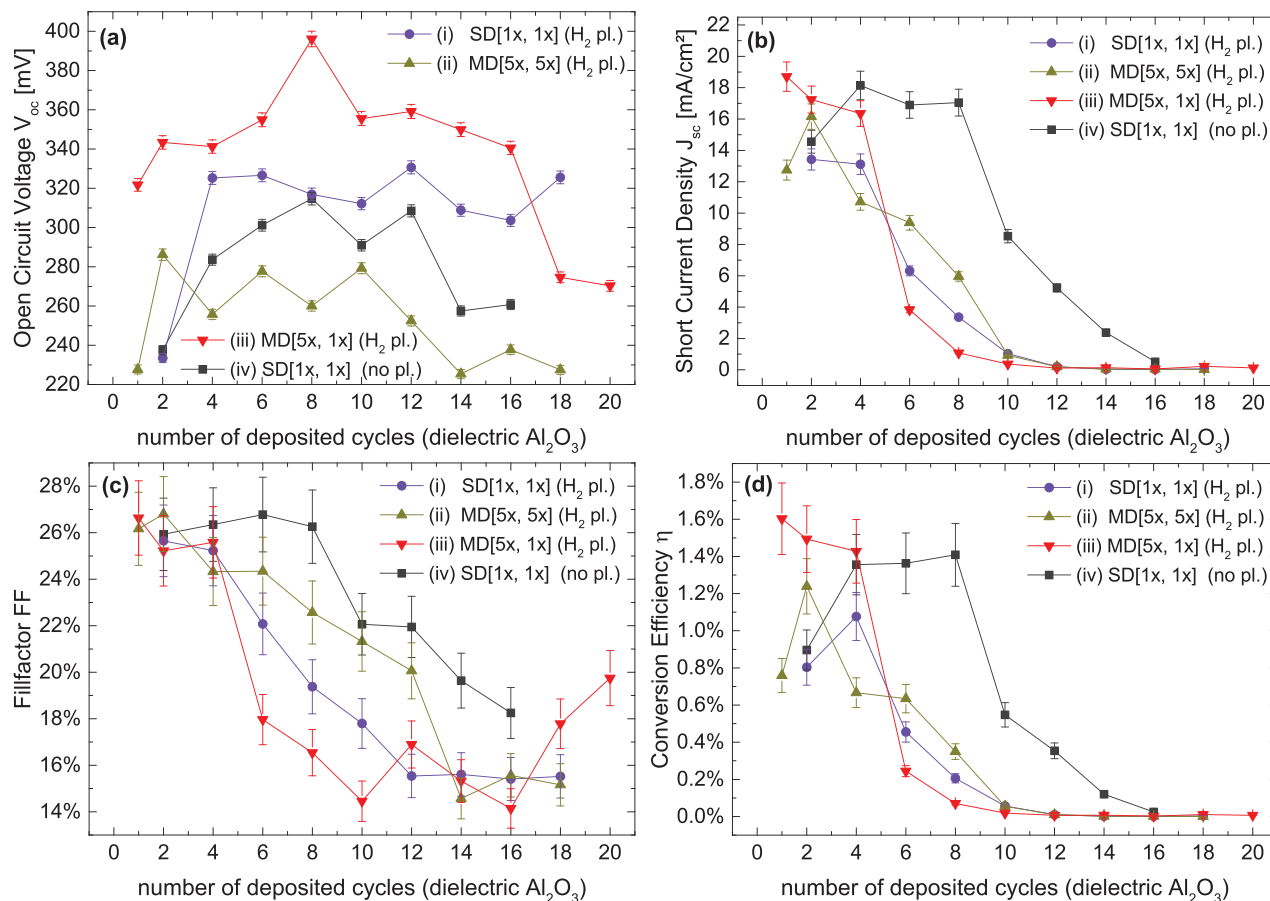


Fig. 1. (Color online) SIS solar cell parameters of dose repetition investigation: (a) open circuit voltage  $V_{oc}$ , (b) short circuit current density  $J_{sc}$ , (c)  $FF$ , and (d) conversion efficiency  $\eta$ . Dielectric Al<sub>2</sub>O<sub>3</sub> layer thickness of 1–20 cycles (growth rate: 0.11 nm/cycle), different precursor dose repetition: (i) single dose [1× TMA and purge, 1× O<sub>2</sub> plasma and purge] (H<sub>2</sub> plasma pretreatment) (SD[1×, 1×] (H<sub>2</sub> pl.)), (ii) multidose [5× TMA and purge, 5× O<sub>2</sub> plasma and purge] (H<sub>2</sub> plasma pretreatment) (MD[5×, 5×] (H<sub>2</sub> pl.)), (iii) multidose [5× TMA and purge, 1× O<sub>2</sub> plasma and purge] (H<sub>2</sub> plasma pretreatment) (MD[5×, 1×] (H<sub>2</sub> pl.)), and (iv) single dose [1× TMA and purge, 1× O<sub>2</sub> plasma and purge] (no plasma pretreatment) (SD[1×, 1×] (no pl.)).

no plasma, and (4) “O<sub>2</sub> and H<sub>2</sub> plasma” were performed before the deposition of Al<sub>2</sub>O<sub>3</sub>. The number of cycles of Al<sub>2</sub>O<sub>3</sub> was altered between 0 and 10. The solar cell parameters of the different plasma pretreatments are shown in Fig. 2.

The open circuit voltage  $V_{oc}$  curves show a significant shift according to the pretreatment. The (1) O<sub>2</sub> plasma curve is discontinuous on the lowest level as compared to the others.  $V_{oc}$  increases in the order of (3) no plasma, (4) O<sub>2</sub> and H<sub>2</sub> plasma, and (2) H<sub>2</sub> plasma.  $V_{oc}$  of (2) H<sub>2</sub> plasma achieves up to 400 mV. (3) no plasma and (4) O<sub>2</sub> and H<sub>2</sub> plasma curves have approximately the same values above 5 cycles.

The short circuit current density  $J_{sc}$  curves show two significant differences: (2) H<sub>2</sub> plasma and (4) O<sub>2</sub> and H<sub>2</sub> plasma pretreated cells remains on a constant level and decrease sharply above 3 and 5 cycles, respectively. In contrary to that,  $J_{sc}$  of (3) no plasma and (1) O<sub>2</sub> plasma slightly increase up to 6 cycles and slightly decrease above. The highest achieved  $J_{sc}$  of (1) O<sub>2</sub> plasma and (3) no plasma are 10–12 mA/cm<sup>2</sup> and 16–20 mA/cm<sup>2</sup>, respectively.  $J_{sc}$  of (2) H<sub>2</sub> plasma and (4) O<sub>2</sub> and H<sub>2</sub> plasma achieves up to 18 and 20 mA/cm<sup>2</sup> in the range of 0–5 and 0–3 cycles, respectively.

The  $FF$  remains in every case of plasma pretreatment around 26% below 5 cycles. Above 5 cycles the (2) H<sub>2</sub> plasma curve decreases most intensively and thereupon (4) O<sub>2</sub> and H<sub>2</sub> plasma and (1) O<sub>2</sub> plasma. (3) no plasma curve decreases at last.

The progressions of conversion efficiencies  $\eta$  correspond approximately to that of  $J_{sc}$ . (1) O<sub>2</sub> plasma achieves 0.7%, (2) H<sub>2</sub> plasma 1.7%, (3) no plasma 1.8%, and (4) O<sub>2</sub> and H<sub>2</sub> plasma 1.5% conversion efficiency.

TEM was performed on cross-sectional SIS solar cells to investigate the influence of plasma pretreatment on the Si/Al<sub>2</sub>O<sub>3</sub> interface. As described before in this section the silicon substrates have been pretreated with (1) O<sub>2</sub> plasma, (2) H<sub>2</sub> plasma, (3) no plasma, and (4) O<sub>2</sub> and H<sub>2</sub> plasma, and immediately covered with 10 cycles Al<sub>2</sub>O<sub>3</sub> and a Al:ZnO. The TEM images are presented in Fig. 3. The thicknesses of the Al<sub>2</sub>O<sub>3</sub> layers were determined from the TEM images and summarized in Table II.

TEM images clearly show the crystal structure of the silicon substrate and on top of that the bright amorphous dielectric Al<sub>2</sub>O<sub>3</sub> layer. The TEM investigation was not able to differentiate between Al<sub>2</sub>O<sub>3</sub> and a SiO<sub>x</sub> layer, which was created on the silicon substrate during the ALD deposition

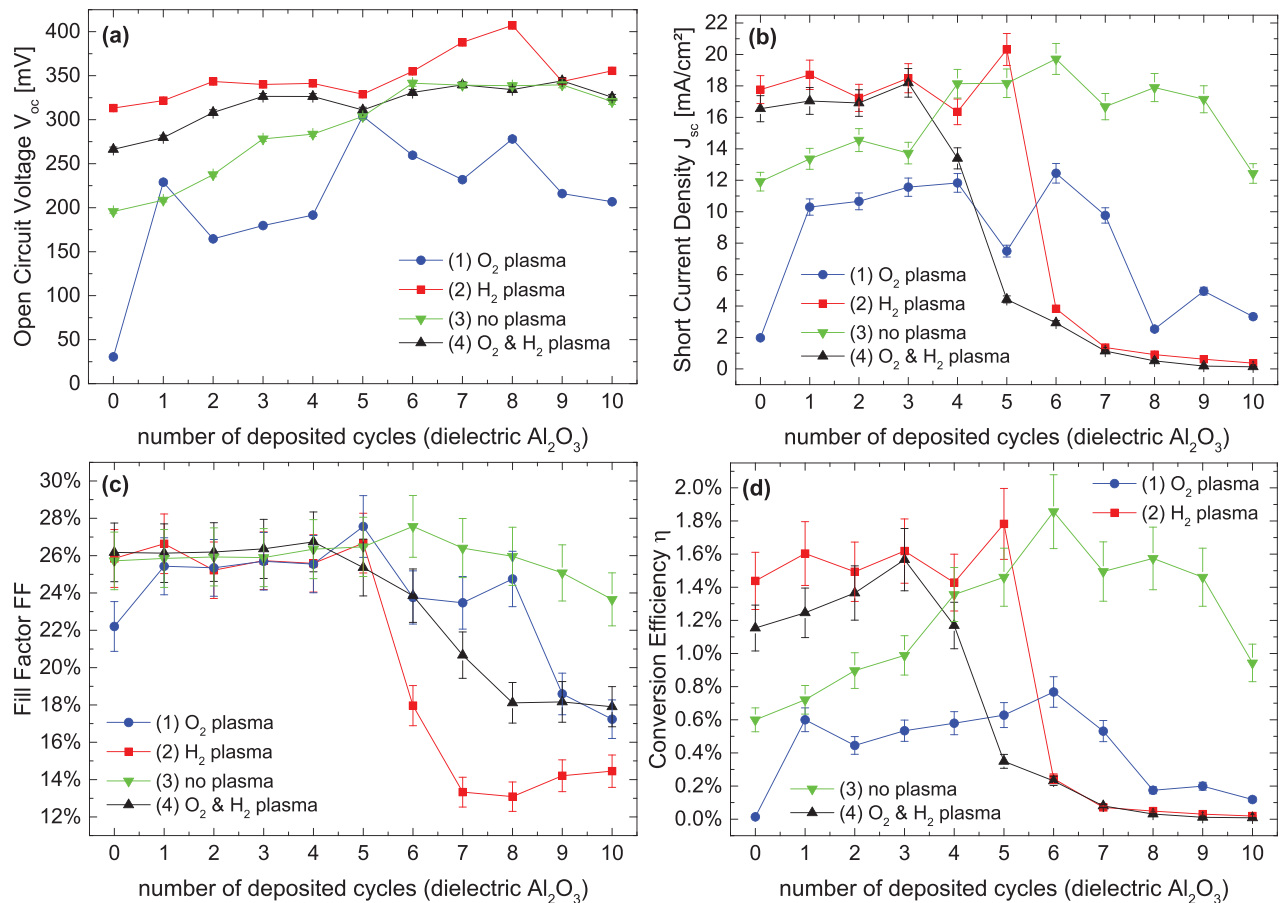


Fig. 2. (Color online) SIS solar cell parameters of plasma pretreatment investigation: (a) open circuit voltage  $V_{oc}$ , (b) short circuit current density  $J_{sc}$ , (c)  $FF$ , and (d) conversion efficiency  $\eta$ , dielectric Al<sub>2</sub>O<sub>3</sub> layer thickness of 0–10 cycles (growth rate: 0.11 nm/cycle), used dose repetition (iii) multidose [5× TMA and purge, 1× O<sub>2</sub> plasma and purge] (H<sub>2</sub> plasma pretreatment) (cf. Fig. 1) for Al<sub>2</sub>O<sub>3</sub> deposition, instantly plasma pretreatment before dielectric Al<sub>2</sub>O<sub>3</sub> deposition: (1) 15s O<sub>2</sub> plasma, (2) 15s H<sub>2</sub> plasma, (3) no plasma, and (4) 15s O<sub>2</sub> plasma and 15s H<sub>2</sub> plasma.

process. Because of that, the dielectric layer here is labeled with “SiO<sub>x</sub>/Al<sub>2</sub>O<sub>3</sub>.” On top of SiO<sub>x</sub>/Al<sub>2</sub>O<sub>3</sub> layer the typical polycrystalline structure of the Al:ZnO front contact is observed.<sup>38–40</sup> The interface between c-Si and SiO<sub>x</sub>/Al<sub>2</sub>O<sub>3</sub> is very sharp. The interface between SiO<sub>x</sub>/Al<sub>2</sub>O<sub>3</sub> and Al:ZnO is more diffuse (Fig. 3). The green line indicates the Si-SiO<sub>x</sub>/Al<sub>2</sub>O<sub>3</sub> interface and the orange and the yellow lines the interface between SiO<sub>x</sub>/Al<sub>2</sub>O<sub>3</sub> and Al:ZnO (Fig. 3).

Comparing the SiO<sub>x</sub>/Al<sub>2</sub>O<sub>3</sub> layer thicknesses with the plasma pretreatment shows that (2) H<sub>2</sub> plasma (1.6–1.9 nm) and (3) no plasma (1.7–2.0 nm) approximately lead to the same thickness. In case (4) O<sub>2</sub> and H<sub>2</sub> plasma (2.0–2.4 nm) and (1) O<sub>2</sub> plasma (2.4–3.0 nm) pretreated, the SiO<sub>x</sub>/Al<sub>2</sub>O<sub>3</sub> layers are significantly thicker than otherwise (Fig. 3 and Table II). The deposition of 10 cycles Al<sub>2</sub>O<sub>3</sub> with a growth rate of 0.11 nm/cycle should lead to a thickness of 1.1 nm. The difference ( $\Delta d_{\min-SiO_x}$ ) of expected and measured thicknesses is given in Table II.

A dependency between the type of plasma pretreatment and the thickness of diffused area at the SiO<sub>x</sub>/Al<sub>2</sub>O<sub>3</sub>/Al:ZnO interfaces are not visible except for (1) O<sub>2</sub> plasma (cf. Table II). There the diffusion area is marginally thicker than in the other cases. In all four cases, the layer thickness is rather uniform within the observed area.

The leakage current density  $J_{Leak}$  at a reverse bias voltage of  $-0.5$  V and shunt resistance  $R_{SH}$  were measured according to the deposited Al<sub>2</sub>O<sub>3</sub> cycles and the four different plasma pretreatment cases (Fig. 4). The (2) H<sub>2</sub> plasma pretreated cells show the lowest and most constant values in the order of  $10^{-3}$  mA/cm<sup>2</sup> ( $1.2 \times 10^5 \Omega/cm^2 \leq R_{SH} \leq 1.3 \times 10^6 \Omega/cm^2$ ). The  $J_{Leak}$  for the series (3) no plasma and (4) O<sub>2</sub> and H<sub>2</sub> plasma was observed to be  $10^{-2}$  and  $10^{-3}$  mA/cm<sup>2</sup> ( $2.0 \times 10^4 \Omega/cm^2 \leq R_{SH} \leq 4.4 \times 10^5 \Omega/cm^2$  and  $8.0 \times 10^4 \Omega/cm^2 \leq R_{SH} \leq 1.4 \times 10^6 \Omega/cm^2$ ), respectively. The (1) O<sub>2</sub> plasma pretreated solar cells with 2–10 cycles exhibit a  $J_{Leak}$  in the order of  $10^{-2}$  mA/cm<sup>2</sup> ( $8.8 \times 10^3 \Omega/cm^2 \leq R_{SH} \leq 9.6 \times 10^4 \Omega/cm^2$ ). With decreasing of deposited Al<sub>2</sub>O<sub>3</sub> cycles  $J_{Leak}$  increases till 9.27 mA/cm<sup>2</sup> ( $R_{SH} = 1.0 \times 10^2 \Omega/cm^2$ ) at 0 cycles.

A special case represents the absence of a dielectric layer between silicon and Al:ZnO. This case is given by the 0 cycle deposition of dielectric Al<sub>2</sub>O<sub>3</sub> (cf. Fig. 2). For a more detailed observation of plasma pretreatment effects, the current–voltage (I–V) characteristic of (1) O<sub>2</sub> plasma, (2) H<sub>2</sub> plasma, and (3) no plasma pretreated solar cells under dark and illumination conditions are plotted in Fig. 5. I–V characteristic under dark condition of (1) O<sub>2</sub> plasma shows a high dark current under reverse bias. In case of (2) H<sub>2</sub> plasma and

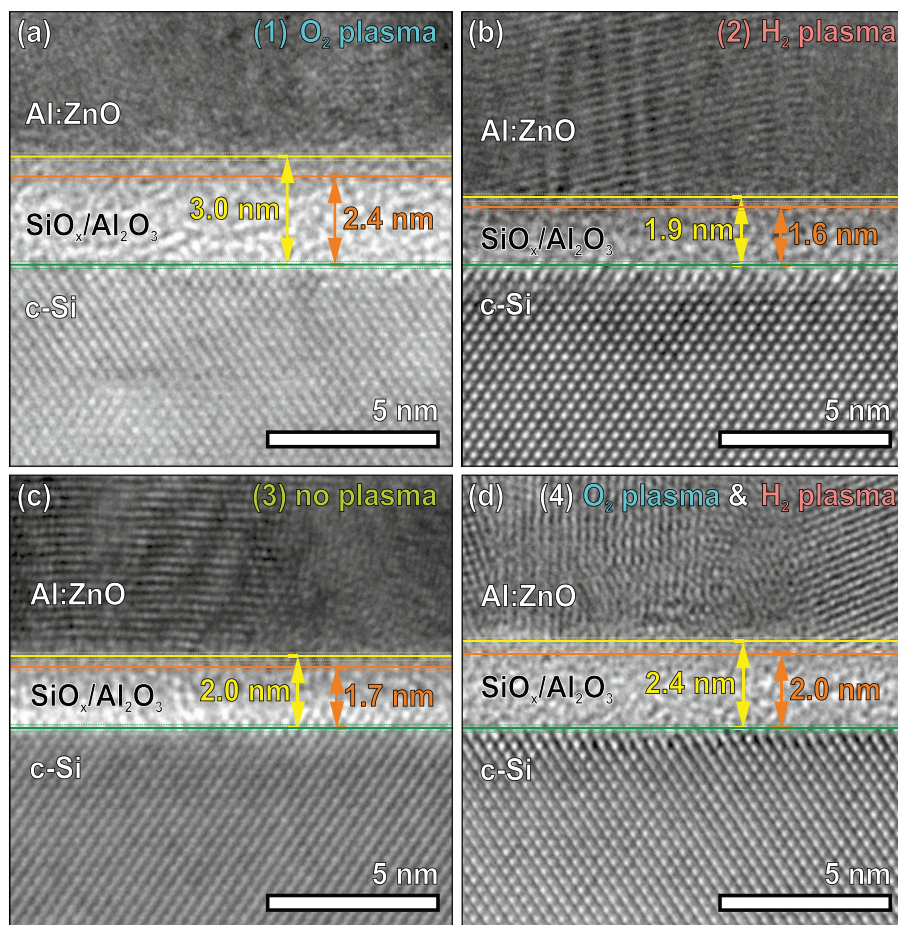


FIG. 3. (Color online) TEM cross-sectional images of  $\text{SiO}_x/\text{Al}_2\text{O}_3$  layer, 10 cycles  $\text{Al}_2\text{O}_3$  deposited, instant plasma pretreatment before  $\text{Al}_2\text{O}_3$  deposition: (1) 15s  $\text{O}_2$  plasma, (2) 15s  $\text{H}_2$  plasma, (3) no plasma, and (4) 15s  $\text{O}_2$  plasma and 15s  $\text{H}_2$  plasma.

(3) no plasma and the reverse current is almost zero ( $10^{-3} \text{ mA/cm}^2$  and  $10^{-2} \text{ mA/cm}^2$ ). Under illumination the (1)  $\text{O}_2$  plasma curve bends up with increasing voltage before the (3) no plasma and (2)  $\text{H}_2$  plasma curves. This directly results in low values of fill factor,  $V_{oc}$  and  $J_{sc}$  of (1)  $\text{O}_2$  plasma and high of (2)  $\text{H}_2$  plasma, because all three curves show a close similarity of slope.

### C. Discussion

The repetition of precursor dose steps significantly influences the solar cell parameters (Fig. 1). This becomes apparent by comparing the single- and multidose application as

TABLE II. Thicknesses of  $\text{SiO}_x/\text{Al}_2\text{O}_3$  layer between c-Si and Al:ZnO by TEM images (cf. Fig. 3) and minimum  $\text{SiO}_x$  layer thicknesses result from growth rate [10 cycles  $\times$  0.11 nm/cycles = 1.1 nm (max. possible  $\text{Al}_2\text{O}_3$  thickness)].

Plasma	$d_{\min}$ (nm)	$d_{\max}$ (nm)	$\Delta d$ (nm)	$\Delta d_{\min-\text{SiO}_x}$ (nm)
(1) $\text{O}_2$ -plasma	2.4	3.0	$\pm 0.2$	1.3
(2) $\text{H}_2$ -plasma	1.6	1.9		0.5
(3) No plasma	1.7	2.0		0.6
(4) $\text{O}_2$ and $\text{H}_2$ plasma	2.0	2.4		0.9

depicted in Fig. 1–(i–iii). Just the repetition of the TMA dose step (iii) MD[5 $\times$ , 1 $\times$ ] ( $\text{H}_2$  pl.) causes an increase in  $J_{sc}$  and particularly in  $V_{oc}$ . However, a degradation is observed by additionally repeating the  $\text{O}_2$  plasma dose step (ii) MD[5 $\times$ , 5 $\times$ ] ( $\text{H}_2$  pl.). Xu *et al.*<sup>41</sup> report a decrease of  $\text{SiO}_2$  interface layer generation by a TMA treatment of 3600s

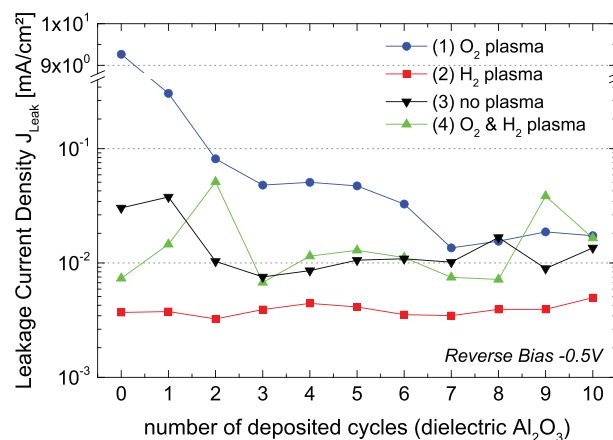


FIG. 4. (Color online) Leakage current density  $J_{Leak}$  at  $-0.5 \text{ V}$  reverse bias of (1) 15s  $\text{O}_2$  plasma, (2) 15s  $\text{H}_2$  plasma, (3) no plasma, and (4) 15s  $\text{O}_2$  plasma and 15s  $\text{H}_2$  plasma pretreated solar cells according to deposited cycles of dielectric  $\text{Al}_2\text{O}_3$  layer (cf. Fig. 2).



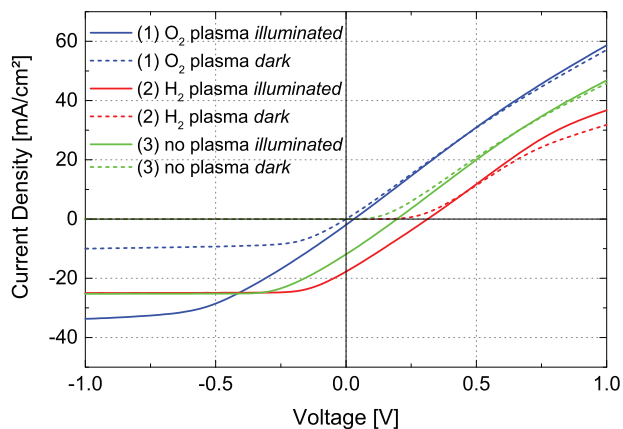


Fig. 5. (Color online) Current–voltage characteristic of dark and illuminated solar cells without deposited of dielectric  $\text{Al}_2\text{O}_3$  layer (0 cycles, cf. Fig. 2) and different plasma pretreatments of (1)  $\text{O}_2$  plasma, (2)  $\text{H}_2$  plasma, and (3) no plasma.

before the  $\text{Al}_2\text{O}_3$  ALD. A repetition of the TMA dose step could have the same effect. TMA molecules, adsorbed on silicon, protect against oxygen. The more the surface is saturated by TMA the less oxidation of silicon occurs. This is indicated by a decrease of  $V_{oc}$  and  $J_{sc}$  with increasing oxidation of the silicon interface. However, this behavior appears to prevent silicon insufficiently against an oxidation in case of  $\text{O}_2$  plasma step repetition (Fig. 1, (ii) MD[5 $\times$ , 5 $\times$ ] ( $\text{H}_2$  pl.)).

TEM was applied to investigate the influence of plasma pretreatment on the Si/ $\text{Al}_2\text{O}_3$  interface (Fig. 3). The deposited 10 cycles of  $\text{Al}_2\text{O}_3$  should lead to a maximum thickness of 1.1 nm. Consequently, the increased thickness of the layer is the result of an oxidation of silicon before or during the deposition process.

The thickness difference between (1)  $\text{O}_2$  plasma and (3) no plasma (Fig. 3) can be explained by an additional oxidation of the silicon surface during the  $\text{O}_2$  plasma pretreatment. However, this explains the difference in thicknesses between (1)  $\text{O}_2$  plasma and (4)  $\text{O}_2$  and  $\text{H}_2$  plasma insufficiently. Let us assume that no increase in thickness during a  $\text{H}_2$  plasma pretreatment occurs [(2)  $\text{H}_2$  plasma]. A few monolayers of  $\text{SiO}_x$  are generated during the  $\text{O}_2$  plasma pretreatment step in case (1)  $\text{O}_2$  plasma and (4)  $\text{O}_2$  and  $\text{H}_2$  plasma. Consequently in case (1)  $\text{O}_2$  plasma a continuing oxidation of silicon occurs. This is prevented by an additional  $\text{H}_2$  plasma pretreatment [(4)  $\text{O}_2$  and  $\text{H}_2$  plasma].

The initial growth behavior in ALD can be described by the number of necessary cycles until a closed layer was formed and a constant growth rate was achieved. This significantly depends on the adsorption behavior of the first precursor (here TMA) on the surface and can lead to a marginal decrease in the deposited layer thickness due to a number of lost cycles. The number of lost cycles has particular influence on very thin layers with only a few number of deposition cycles. A treatment of the silicon surface by hydrogen plasma leads to a hydrogen termination of the surface.<sup>42</sup> This termination improves the initial growth behavior of  $\text{Al}_2\text{O}_3$  and reduces and prevents silicon surface

oxidation.<sup>43,44</sup> Thus, on a hydrogen terminated surface, a short initial growth phase (or small number of lost cycles) should result in a thicker layer of  $\text{Al}_2\text{O}_3$  in comparison to a none-terminated surface. Consequently, the (2)  $\text{H}_2$  plasma layer should be thicker than the (3) no plasma layer. However, the thickness of (2)  $\text{H}_2$  plasma and (3) no plasma is nearly the same. This implies a different content of  $\text{SiO}_x$  and  $\text{Al}_2\text{O}_3$  in the  $\text{SiO}_x/\text{Al}_2\text{O}_3$  layer. In case (3) no plasma, the  $\text{SiO}_x$  content is large and the  $\text{Al}_2\text{O}_3$  content is small. In case (2)  $\text{H}_2$  plasma, the ratio is reversed. A high content of  $\text{SiO}_x$  could be caused by a large number of lost cycles and a strong silicon oxidation. A high  $\text{Al}_2\text{O}_3$  content could be caused by a small number of lost cycles and a fast initial growth that reduces silicon oxidation.

Based on that, the shift of the open circuit voltage  $V_{oc}$  [Fig. 2(a)] correlates directly to the  $\text{SiO}_x$  layer thickness. The induced  $\text{SiO}_x$  generation by an oxygen plasma pretreatment has only marginal influence [(4)  $\text{O}_2$  and  $\text{H}_2$  plasma] in contrast to that induced by worse initial growth behavior [(1)  $\text{O}_2$  plasma]. The short circuit current density  $J_{sc}$  [Fig. 2(b)] of (1)  $\text{O}_2$  plasma and (3) no plasma increase and decrease slightly over the number of cycles.  $J_{sc}$  of (2)  $\text{H}_2$  plasma and (4)  $\text{O}_2$  and  $\text{H}_2$  plasma decrease intensely above 5 and 3 cycles, respectively, from a constant value. Above this point, the tunneling probability drastically decreases, because the dielectric layer becomes too thick. (1)  $\text{O}_2$  plasma and (3) no plasma leads to an insufficient thickness to pass over this limit in the observed range. That also implies worse initial growth behavior. Theoretical calculations of Shewchun *et al.*<sup>17</sup> on the behavior of  $J_{sc}$  related to dielectric layer thickness demonstrate also this strongly decrease after exceeding a thickness limit (1.8 nm for  $\text{SiO}_2$ ). During the  $\text{O}_2$  plasma pretreatment step of (4)  $\text{O}_2$  and  $\text{H}_2$  plasma a  $\text{SiO}_x$  layer with an equivalent thickness of 2 cycles  $\text{Al}_2\text{O}_3$  was generated. Consequently, in consideration of layer thicknesses (Fig. 3), the decrease of  $J_{sc}$  at the same numbers of cycles for (2)  $\text{H}_2$  plasma and (3) no plasma or at lower number of cycles for (1)  $\text{O}_2$  plasma and (4)  $\text{O}_2$  and  $\text{H}_2$  plasma should occur.

The behavior of the  $FF$  shows a decrease of (1)  $\text{O}_2$  plasma, (2)  $\text{H}_2$  plasma, and (4)  $\text{O}_2$  and  $\text{H}_2$  plasma from a stable level of 26% after exceeding 5 cycles. The decrease is proportional to the decrease of  $J_{sc}$ .  $FF$  only achieves a maximum of nearly 26% that is caused mainly by the material composition. The absence of a front grid can result in a large series resistance and decreases the  $FF$  as well. Bethge *et al.* investigated further dielectrics and achieved  $FF$  values of 40%–71% depending on used materials.<sup>32</sup>

The case of 0 cycles is a special case (Figs. 2 and 5). It is indicated that silicon and Al:ZnO generate a functional photovoltaic junction without an additional dielectric. If the reason would be the generation of  $\text{SiO}_x$  during Al:ZnO deposition, then (1)  $\text{O}_2$  plasma pretreatment would offer the best requirements for a Si/ $\text{SiO}_x$ /Al:ZnO junction. However, (1)  $\text{O}_2$  plasma has the lowest  $V_{oc}$  and  $J_{sc}$  values. Highly doped  $n^+$ -Al:ZnO and low doped  $n$ -Si form an abrupt  $n$ - $n^+$  heterojunction, that generates an energy barrier at the interface.<sup>45</sup> In any case, some ML  $\text{SiO}_x$  were generated during deposition, as it was discussed before.



The quality of the interface plays an important role for the junction behavior, especially the probability of charge carriers tunneling through the junction. Surface states and interface defects like fixed charges  $Q_f$  and interface traps  $D_{it}$  are generated by oxidation states and dangling bonds, respectively. The  $\text{SiO}_x$  layer formed during (1)  $\text{O}_2$  plasma pretreatment (0 cycles) allows charge carriers the transition between Si and Al:ZnO in both directions. By introduction of an  $\text{Al}_2\text{O}_3$  layer, the transition in reverse bias direction (Al:ZnO in Si) drastically decreases while transition in the other direction still occurs (cf. Figs. 2 and 4, 0–2 cycles). However, introducing hydrogen into the interface, like in case (2)  $\text{H}_2$  plasma and (4)  $\text{O}_2$  and  $\text{H}_2$  plasma, the formed  $\text{SiO}_x$  layer allows only a marginal leakage current density  $J_{\text{Leak}}$ .

Dangling bonds at Si interface and in the formed  $\text{SiO}_x$  layer generate trap states  $D_{it}$  within the bandgap that allow trap-assisted tunneling through the barrier.<sup>46–48</sup> Hydrogen can passivate these dangling bonds at the interfaces and in  $\text{SiO}_x$ .<sup>49–52</sup> Investigations of metal-oxide-semiconductor (MOS) structures show that by performing a hydrogen treatment the  $D_{it}$  can be reduced up to one magnitude.<sup>53</sup> As a result in MOS structures the leakage current density  $J_{\text{Leak}}$  was reduced.<sup>54,55</sup> In due consideration the hydrogen plasma pretreatment effects the same interface passivation.

It was deduced before that in case (1)  $\text{O}_2$  plasma and (3) no plasma the content of  $\text{SiO}_x$  in the  $\text{SiO}_x/\text{Al}_2\text{O}_3$  interface is larger than in (2)  $\text{H}_2$  plasma and (4)  $\text{O}_2$  and  $\text{H}_2$  plasma. It is assumed that the  $\text{SiO}_x$  layer, formed during plasma pretreatment and deposition of  $\text{Al}_2\text{O}_3$  in case (1)  $\text{O}_2$  plasma and (3) no plasma, which is not hydrogen passivated, contains a large number of trap states  $D_{it}$ . Because charge carriers are able to tunnel in these trap states, the thickness of the  $\text{SiO}_x$  layer do not act as part of the dielectric layer thickness. In consideration of a larger number of lost cycles (see above), as a result, the threshold point, where  $J_{\text{sc}}$  decreases because of a too thick dielectric layer, is shifted from 3 and 5 cycles, respectively, to above 10 cycles.

Based on this, the  $\text{SiO}_x/\text{Al}_2\text{O}_3$  interface layer in case (1)  $\text{O}_2$  plasma has the highest value of  $D_{it}$  and contains the highest fraction of  $\text{SiO}_x$ . As a result, the SIS junction behavior becomes more unpredictable and less reproducible. This may be the reason for the comparatively high fluctuation in  $V_{\text{oc}}$  and  $J_{\text{sc}}$  values of (1)  $\text{O}_2$  plasma (Fig. 2).

The conversion efficiency  $\eta$  of solar cells, calculated from  $V_{\text{oc}}$ ,  $J_{\text{sc}}$ , and  $FF$ , of (2)  $\text{H}_2$  plasma pretreated achieves the highest values in the range below 5 cycles. Only (3) no plasma achieves a marginal higher value at 6 cycles, where the  $FF$  of (3) no plasma also achieves its maximum. Due to the discontinuity of  $\eta$  at this point, it cannot be concluded that higher conversion efficiencies can be achieved by no plasma pretreatment. Bethge *et al.*<sup>32</sup> used thermal ALD for deposition of several materials like  $\text{Al}_2\text{O}_3$  as dielectric layer between p-Si and Al:ZnO. With lanthanum oxide ( $\text{La}_2\text{O}_3$ ) a conversion efficiency of 8% was achieved. In case of  $\text{Al}_2\text{O}_3$  the leakage current density was in  $\text{mA}/\text{cm}^2$  range. They observed a diffusion of metal atoms between  $\text{Al}_2\text{O}_3$  and Al:ZnO layer and deduced interface defects and trap-assisted

tunneling. In general using thermal instead of plasma-enhanced ALD can reduce the  $\text{SiO}_x$  generation. The influence of temperature on the interface formation was not considered here as well. However, a  $\text{H}_2$  plasma pretreatment improves the growth behavior of the used dielectric layer, passivates interface dangling bond and result in higher open circuit voltages  $V_{\text{oc}}$  and short circuit current densities  $J_{\text{sc}}$ .

#### IV. SUMMARY AND CONCLUSIONS

SIS solar cells with n-Si/ $\text{Al}_2\text{O}_3$ /Al:ZnO layer stacks were realized on single crystalline n-type Si(100) 1–10  $\Omega\text{cm}$  substrates by plasma-enhanced atomic layer deposition. The number of deposited cycles of  $\text{Al}_2\text{O}_3$  was altered between 0 and 20. Single precursor dose steps were repeated during the  $\text{Al}_2\text{O}_3$  deposition. Open circuit voltage ( $V_{\text{oc}}$ ), short circuit current density ( $J_{\text{sc}}$ ),  $FF$ , and conversion efficiency ( $\eta$ ) were investigated. The repetition of TMA dose step leads to an improvement of cell parameters, mainly  $V_{\text{oc}}$  ( $V_{\text{oc}} = 340\text{--}400$  mV,  $J_{\text{sc}} = 16\text{--}19$   $\text{mA}/\text{cm}^2$ ,  $\eta = 1.4\%\text{--}1.6\%$ ). The repetition of oxygen plasma steps causes a decrease of cell parameters ( $V_{\text{oc}} = 260\text{--}280$  mV,  $J_{\text{sc}} = 11\text{--}16$   $\text{mA}/\text{cm}^2$ , and  $\eta = 0.8\%\text{--}1.2\%$ ) compared to those of none repetition ( $V_{\text{oc}} = 310\text{--}330$  mV,  $J_{\text{sc}} = 13$   $\text{mA}/\text{cm}^2$ , and  $\eta = 0.8\%\text{--}1.2\%$ ).

Pretreatments of the silicon surface by  $\text{O}_2$ ,  $\text{H}_2$ , and  $\text{O}_2$  and  $\text{H}_2$  plasma as a sequence, immediately before dielectric  $\text{Al}_2\text{O}_3$  deposition, was performed. The plasma pretreatment affects differently the measured solar cell parameters. TEM investigations were performed on the Si/ $\text{Al}_2\text{O}_3$  interface. The results show a high silicon oxide generation at the interface by  $\text{O}_2$  plasma pretreatment and a low one by  $\text{H}_2$  plasma. This oxidation is a slight result of the  $\text{O}_2$  plasma pretreatment. The oxidation is mainly caused by different initial growth behaviors of  $\text{Al}_2\text{O}_3$ . The initial growth is delayed by  $\text{O}_2$  plasma and accelerated by  $\text{H}_2$  plasma pretreatment. The performance of  $\text{H}_2$  plasma pretreated solar cells increase ( $V_{\text{oc}} = 340$  mV,  $J_{\text{sc}} = 20$   $\text{mA}/\text{cm}^2$ , and  $\eta = 1.8\%$ ), that of  $\text{O}_2$  plasma pretreated decrease ( $V_{\text{oc}} = 250$  mV,  $J_{\text{sc}} = 12$   $\text{mA}/\text{cm}^2$ , and  $\eta = 0.7\%$ ).

A more detailed examination of solar cell parameters and TEM images show several effects, which affect solar cell parameters. The apparent effect is the Si/ $\text{Al}_2\text{O}_3$  interface oxidation by different plasma pretreatments. Interface states and defects have important influence on solar cell performance. The formed  $\text{SiO}_x$  layer during  $\text{O}_2$  plasma pretreatment and deposition of dielectric  $\text{Al}_2\text{O}_3$  layer contains a high value of trap states in due to the presence of dangling bonds. The interface traps degrade the solar cells.

It is assumed that a  $\text{H}_2$  plasma pretreatment passivates the dangling bonds and reduces the trap states density. Also, it reduces the generation of  $\text{SiO}_x$  by an improvement of initial growth behavior of dielectric  $\text{Al}_2\text{O}_3$  layer. As a result, a higher performance of semiconductor–insulator–semiconductor solar cell can be achieved.

#### ACKNOWLEDGMENTS

The authors thank Silke Neuhaus for the very time-consuming carving of the chips and wafers. This work was

supported by the National Science Foundation of Germany (DFG) under German–Russian Grant No. SI1893/4-1 and German–Kazakh Grant No. SI1893/5-1.

- <sup>1</sup>M. A. Green, K. Emery, Y. Hishikawa, and W. Warta, *Prog. Photovoltaics* **19**, 84 (2011).
- <sup>2</sup>M. A. Green, K. Emery, Y. Hishikawa, W. Warta, and E. D. Dunlop, *Prog. Photovoltaics* **20**, 12 (2012).
- <sup>3</sup>V. Sivakov, G. Andrä, A. Gawlik, A. Berger, J. Plentz, F. Falk, and S. H. Christiansen, *Nano Lett.* **9**, 1549 (2009).
- <sup>4</sup>T. Stelzner, M. Pietsch, G. Andrä, F. Falk, E. Ose, and S. Christiansen, *Nanotechnology* **19**, 295203 (2008).
- <sup>5</sup>B. Tian, X. Zheng, T. J. Kempa, Y. Fang, N. Yu, G. Yu, J. Huang, and C. M. Lieber, *Nature* **449**, 885 (2007).
- <sup>6</sup>M. D. Kelzenberg, D. B. Turner-Evans, B. M. Kayes, M. A. Filler, M. C. Putnam, N. S. Lewis, and H. A. Atwater, *Nano Lett.* **8**, 710 (2008).
- <sup>7</sup>E. C. Garnett and P. Yang, *J. Am. Chem. Soc.* **130**, 9224 (2008).
- <sup>8</sup>O. Gunawan and S. Guha, *Sol. Energy Mater. Sol. Cells* **93**, 1388 (2009).
- <sup>9</sup>M. Law, L. E. Greene, J. C. Johnson, R. Saykally, and P. Yang, *Nat. Mater.* **4**, 455 (2005).
- <sup>10</sup>L. Tsakalakos, J. Balch, J. Fronheiser, B. A. Korevaar, O. Sulima, and J. Rand, *Appl. Phys. Lett.* **91**, 233117 (2007).
- <sup>11</sup>T. Yamazaki, Y. Uraoka, and T. Fuyuki, *Jpn. J. Appl. Phys.* **45**, 2441 (2006).
- <sup>12</sup>L. Shen, Z. C. Liang, C. F. Liu, T. J. Long, and D. L. Wang, *AIP Adv.* **4**, 027127 (2014).
- <sup>13</sup>M. Schmidt, L. Korte, A. Laades, R. Stangl, C. Schubert, H. Angermann, E. Conrad, and K. v. Maydell, *Thin Solid Films* **515**, 7475 (2007).
- <sup>14</sup>W. A. Anderson and A. E. Delahoy, *Proc. IEEE* **60**, 1457 (1972).
- <sup>15</sup>M. A. Green and J. Shewchun, *Solid State Electron.* **17**, 349 (1974).
- <sup>16</sup>J. Shewchun, R. Singh, and M. A. Green, *J. Appl. Phys.* **48**, 765 (1977).
- <sup>17</sup>J. Shewchun, J. Dubow, A. Myszkowski, and R. Singh, *J. Appl. Phys.* **49**, 855 (1978).
- <sup>18</sup>J. Shewchun, J. Dubow, C. W. Wilmsen, R. Singh, D. Burk, and J. F. Wager, *J. Appl. Phys.* **50**, 2832 (1979).
- <sup>19</sup>W. W. Wenas and S. Riyadi, *Sol. Energy Mater. Sol. Cells* **90**, 3261 (2006).
- <sup>20</sup>H. Kobayashi, T. Ishida, Y. Nakato, and H. Tsubomura, *J. Appl. Phys.* **69**, 1736 (1991).
- <sup>21</sup>H. P. Maruska, A. K. Ghosh, D. J. Eustace, and T. Feng, *J. Appl. Phys.* **54**, 2489 (1983).
- <sup>22</sup>H. Kobayashi, H. Mori, T. Ishida, and Y. Nakato, *J. Appl. Phys.* **77**, 1301 (1995).
- <sup>23</sup>O. Lupan, S. Shishiyanu, V. Ursaki, H. Khallaf, L. Chow, T. Shishiyanu, V. Sontea, E. Monaico, and S. Railean, *Sol. Energy Mater. Sol. Cells* **93**, 1417 (2009).
- <sup>24</sup>S. Dengyuan and G. Baozeng, *J. Phys. D: Appl. Phys.* **42**, 025103 (2009).
- <sup>25</sup>M. Ritala and M. Leskelä, *Handbook of Thin Films* (Academic, Burlington, MA, 2002), pp. 103–159.
- <sup>26</sup>M. Leskelä and M. Ritala, *Thin Solid Films* **409**, 138 (2002).
- <sup>27</sup>K. Grigoras, S. Franssila, and V.-M. Airaksinen, *Thin Solid Films* **516**, 5551 (2008).
- <sup>28</sup>V. Miikkulainen, M. Leskelä, M. Ritala, and R. L. Puurunen, *J. Appl. Phys.* **113**, 021301 (2013).
- <sup>29</sup>S. Ratzsch, K. Ernst-Bernhard, T. Andreas, and S. Adriana, *Nanotechnology* **26**, 024003 (2015).
- <sup>30</sup>J.-S. Na, Q. Peng, G. Scarel, and G. N. Parsons, *Chem. Mater.* **21**, 5585 (2009).
- <sup>31</sup>H. Liu, V. Avrutin, N. Izyumskaya, Ü. Özgür, and H. Morkoç, *Superlattices Microstruct.* **48**, 458 (2010).
- <sup>32</sup>O. Bethge, M. Nobile, S. Abermann, M. Glaser, and E. Bertagnolli, *Sol. Energy Mater. Sol. Cells* **117**, 178 (2013).
- <sup>33</sup>B. Lee *et al.*, *Microelectron. Eng.* **86**, 1658 (2009).
- <sup>34</sup>B. S. Lim, A. Rahtu, P. de Rouffignac, and R. G. Gordon, *Appl. Phys. Lett.* **84**, 3957 (2004).
- <sup>35</sup>S. B. S. Heil, P. Kudlacek, E. Langereis, R. Engeln, M. C. M. van de Sanden, and W. M. M. Kessels, *Appl. Phys. Lett.* **89**, 131505 (2006).
- <sup>36</sup>S.-C. Ha, E. Choi, S.-H. Kim, and J. S. Roh, *Thin Solid Films* **476**, 252 (2005).
- <sup>37</sup>D. Kim, H. Kang, J.-M. Kim, and H. Kim, *Appl. Surf. Sci.* **257**, 3776 (2011).
- <sup>38</sup>S. Keun Kim, C. Seong Hwang, S.-H. Ko Park, and S. Jin Yun, *Thin Solid Films* **478**, 103 (2005).
- <sup>39</sup>D.-J. Lee, H.-M. Kim, J.-Y. Kwon, H. Choi, S.-H. Kim, and K.-B. Kim, *Adv. Funct. Mater.* **21**, 448 (2011).
- <sup>40</sup>T. Dhakal, D. Vanhart, R. Christian, A. Nandur, A. Sharma, and C. R. Westgate, *J. Vac. Sci. Technol. A* **30**, 021202 (2012).
- <sup>41</sup>M. Xu, C. Zhang, S.-J. Ding, H.-L. Lu, W. Chen, Q.-Q. Sun, D. W. Zhang, and L.-K. Wang, *J. Appl. Phys.* **100**, 106101 (2006).
- <sup>42</sup>M. Shinohara, T. Kuwano, Y. Akama, Y. Kimura, M. Niwano, H. Ishida, and R. Hatakeyama, *J. Vac. Sci. Technol. A* **21**, 25 (2003).
- <sup>43</sup>M. M. Frank *et al.*, *Appl. Phys. Lett.* **83**, 740 (2003).
- <sup>44</sup>M. M. Frank, Y. Wang, M.-T. Ho, R. T. Brewer, N. Moumen, and Y. J. Chabal, *J. Electrochem. Soc.* **154**, G44 (2007).
- <sup>45</sup>R. Romero, M. C. López, D. Leinen, F. Martín, and J. R. Ramos-Barrado, *Mater. Sci. Eng. B* **110**, 87 (2004).
- <sup>46</sup>J. Kang, Y.-H. Kim, J. Bang, and K. J. Chang, *Phys. Rev. B* **77**, 195321 (2008).
- <sup>47</sup>M. Houssa, M. Tuominen, M. Naili, V. Afanas'ev, A. Stesmans, S. Haukka, and M. M. Heyns, *J. Appl. Phys.* **87**, 8615 (2000).
- <sup>48</sup>Y. S. Choi, T. Nishida, and S. E. Thompson, *Appl. Phys. Lett.* **92**, 173507 (2008).
- <sup>49</sup>T. Ono, *Phys. Rev. B* **79**, 195326 (2009).
- <sup>50</sup>A. G. Revesz, *J. Electrochem. Soc.* **126**, 122 (1979).
- <sup>51</sup>E. H. Poindexter, *J. Non-Cryst. Solids* **187**, 257 (1995).
- <sup>52</sup>G. Dingemans, W. Beyer, M. C. M. van de Sanden, and W. M. M. Kessels, *Appl. Phys. Lett.* **97**, 152106 (2010).
- <sup>53</sup>I. S. Jeon *et al.*, *Appl. Phys. Lett.* **82**, 1066 (2003).
- <sup>54</sup>H. Wong and H. Iwai, *Microelectron. Eng.* **83**, 1867 (2006).
- <sup>55</sup>Asuha, T. Kobayashi, O. Maida, M. Inoue, M. Takahashi, Y. Todokoro, and H. Kobayashi, *Appl. Phys. Lett.* **81**, 3410 (2002).